A SIMPLE FORCE BALANCE ACCELEROMETER/SEISMOMETER BASED ON A TUNING FORK DISPLACEMENT SENSOR

D. Stuart-Watson and J. Tapson

Department of Electrical Engineering, University of Cape Town, Rondebosch 7701, South Africa

Seismometers and MEMS accelerometers use the force-balance principle to obtain measurements. In these instruments the displacement of a mass object by an unknown force is sensed using a very high-resolution displacement sensor. The position of the object is then stabilised by applying an equal and opposite force to it. The magnitude of the stabilising force is easily measured, and is assumed to be equivalent to the unknown force. These systems are critically dependent on the displacement sensor. In this paper we use a resonant quartz tuning fork as the sensor. The tuning fork is operated so that its oscillation is lightly damped by the proximity of the movable mass object. Changes in the position of the mass object cause changes in the phase of the fork's resonance; this is used as the feedback variable in controlling the mass position. We have developed a novel acceleration sensor using this principle. The mass object is a piezoelectric bimorph diaphragm which is anchored around its perimeter, allowing direct electronic control of the displacement of its centre. The tuning fork is brought very close to the diaphragm centre, and is connected into a self-oscillating feedback circuit which has phase and amplitude as outputs. The diaphragm position is adjusted by a feedback loop, using phase as the feedback variable, to keep it in a constant position with respect to the tuning fork. The measured noise for this sensor is approximately 10.0 mg in a bandwidth of 100 Hz, which is substantially better than equivalent commercial systems.

1. INTRODUCTION

Many instruments work by treating the measurand as a disturbance, and measuring the input required to null that disturbance. Examples are in probe microscopy, where the disturbances are changes to the probe-surface interaction; and in seismometry, where the disturbances are forces applied to a mass by movements of the Earth's surface. This method allows a nonlinear measurement (of the disturbance) to be replaced by a linear measurement (of the balancing action); this in turn allows the construction of systems with very high dynamic range.

A particular case of this type is acceleration measurement. In these systems, the force applied to the system results in an acceleration to a test mass. The mass displacement is sensed, and an opposing (restoring) force is applied to nullify the acceleration. The mass therefore moves in only a vanishingly small zone around the null point. This permits the use of large masses with weak suspensions (to enhance sensitivity), but reduces the need for a long range of travel for such a mass.

Central to this system is the displacement sensor. It must have high resolution and wide bandwidth; but fortunately, it does not require a wide range, as if the system is working correctly, the mass should not in any real sense move at all. In current force-balance systems, it is usual to use a capacitive or optical displacement sensor [1].

Recently, Grober et al [2] have suggested that a quartz crystal tuning fork, oriented so that the mass movement would impinge on one of the tines, could be more sensitive to displacement than any other commonly used method. These tuning forks are widely available as oscillators in quartz watches and timing systems. The relevant parameters for these crystals at resonance are a noise floor of 0.62 pN/Hz, and a mean root square Brownian motion of only 0.32 pm. Closed loop responses of the crystal are also significantly faster than the corresponding open loop responses.

In this paper we describe a novel force-balance sensor, suitable as an accelerometer or wideband seismometer, using a tuning-fork displacement sensor. We discuss the control of such a system, and show that the sensitivity is substantially better than commercially available systems.

2. OVERVIEW

Physically the system is set up inside an aluminium casing. The tuning fork crystal is mounted on a threaded ceramic cylinder. The diaphragm is mounted above the crystal and supported and secured around its outer edge. The threaded cylinder is then turned, moving the tuning fork arms into close proximity with the diaphragm. A rough idea of the physical set up of the system can be seen in figure 1.

Two distinct control loops exist in the set up of the tuning fork seismometer. The control loop to keep the crystal resonating and the control loop to keep the piezoelectric diaphragm at a specific height above the crystal. For both control loops the measured outputs come from the crystal. Of the two outputs, phase and amplitude, the phase response of the crystal will be faster than its amplitude response by a factor of Q.

For this reason the phase between the drive voltage and output voltage is used for the diaphragm height control. The diaphragm height control loop provides the force feedback for the system, and therefore the relative ground acceleration measurement comes from this loop, so therefore speed is more imperative for this control loop. The basic setup of the tuning fork seismometer control systems is also shown in figure 1.

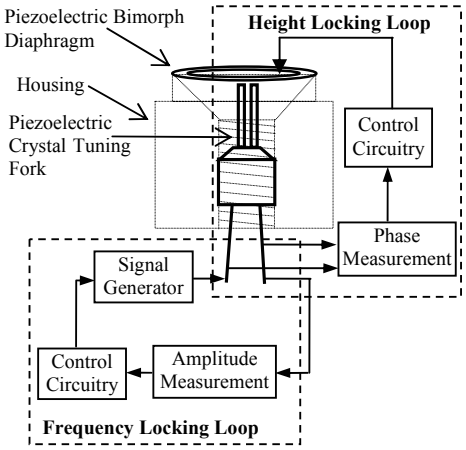

Figure 1: The basic setup of the tuning fork seismometer. Clearly seen are the two control loops present in the system. Besides providing the force feedback mechanism, the diaphragm also forms the mass and spring of the seismometer. Thus the mechanical sensitivity of the device can be determined by the mass of the diaphragm and its spring constant.

3. TUNING FORK DISPLACEMENT SENSOR

In order for the crystal to perform as a displacement sensor it is imperative that it is locked at a frequency somewhere in its resonant band. As mentioned before, the amplitude of the output waveform from the crystal would be used to determine at which frequency the crystal was operating.

The equivalent circuit of the crystal can be described as a simple RLC series circuit in parallel with a package capacitance caused by the electrode plating [2]. The package capacitance affects the operation of the crystal and has an adverse effect on its ability to perform as a displacement sensor. The effect of the package capacitance is reduced by driving another capacitance, of equal value, in parallel with the crystal with the inverse signal used to drive the crystal. As they are equal in value the effect of the one capacitance will cancel out the effect of the other. With the package capacitance negated the crystal behaves like a series RLC circuit with resonant phase and amplitude characteristics seen below in figure 2.

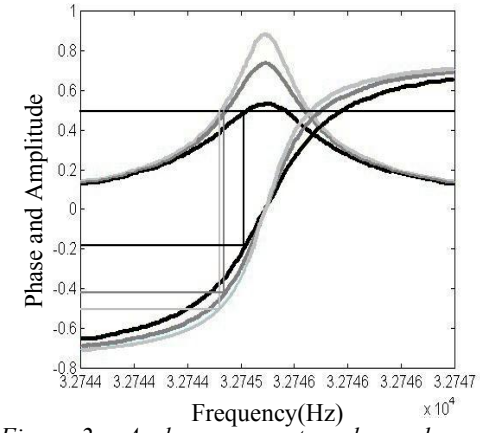

Figure 2 - A clear resonant peak can be seen at about 32745 Hz, and the phase moves from a lagging to a leading phase through the resonant peak. The different coloured lines represent the different levels of damping caused by crystal proximity to a surface. The proximity increases the viscosity of the air, which damps the tuning fork arm movements. This effectively changes the resistance in the equivalent circuit, as resistance is attributed to the arm movement [2]. If the top horizontal line is considered to be the locking amplitude level, the phase and operating frequency changes for each level of damping can be seen. There are two possible operating points for each amplitude, one on either side of the resonant peak. The operating frequency therefore either needs to be swept up from lower frequencies or swept down from higher frequencies to one of the operating points. The offset in resonant frequency from the expected 32768Hz is due to the crystal package having been opened.

To keep the crystal operating at a point in its resonant band, using the amplitude of the output waveform as the control variable, requires that the output waveform amplitude is measured and the crystal operating frequency adjusted accordingly. A basic outline of the system appears in figure 3.

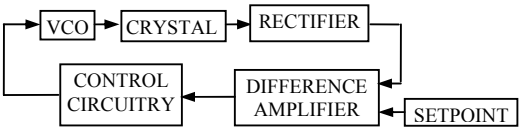

Figure 3 – The basic block diagram for the amplitude control loop. The sine wave producing VCO could be set up to either sweep up or down to the operating point depending on the polarity of the controller output and the initial set up of the VCO. The rectifier measures the amplitude of the output waveform so it can be compared to the set point.

In order to accurately measure phase for the piezoelectric diaphragm controller, it is also important that the two signals that are to be measured

are the same size. Achieving this initially required some dynamic gain control circuitry, which amplified the level of the drive signal to the crystal and the output signal from the crystal by varying amounts so that they were the same size. Although it worked this was a cumbersome complicated process involving many components and extra circuitry.

A different approach to simplify the process was to use the rectified drive signal as the set point to the difference amplifier. This eliminated the need for active gain control, as the system operates at the point where the drive signal and output waveform are the same size. By adding gain to the drive and output signals the frequency at which the system operates can be changed. Furthermore, to reduce the ripple caused by the rectifiers a variable phase shifter is added to the drive signal, so that the two signals can be manipulated to be in phase at the chosen operating frequency. The ripple on the two rectified signals is then cancelled out to produce a cleaner signal for the control circuitry.

When designing the control circuitry, step tests were performed across the whole crystal rectifier combination. This was done so that the time constants present in the rectifiers could also be accounted for in the control of the system. The control block diagram in figure 4 explains the process.

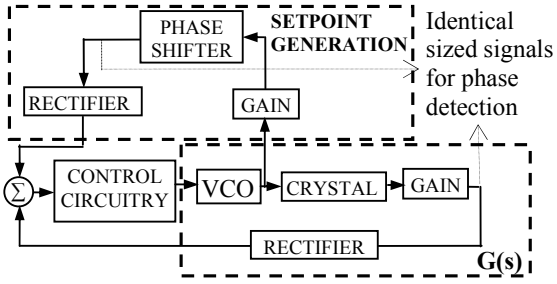

Figure 4 - Control block diagram for the frequency locking loop. Clearly seen is the G(s) for the control system which consists of the crystal with its package capacitance eliminated as well as the VCO, rectifier and the gain. Also seen is the set point generation using the drive signal to the crystal. Step tests were performed across the G(s) combination so that the control circuitry could be designed.

A number of step tests were performed and the results were averaged to determine the characteristics that were to be used to design the controller. The averaged results of the step tests and the characteristic response for the open loop system appear in figure 5.

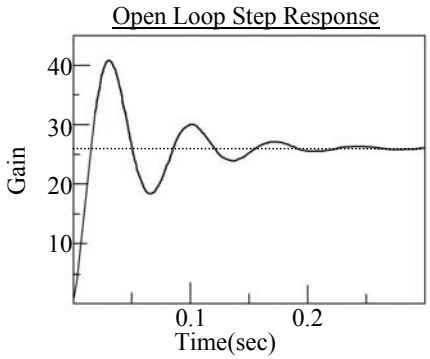

Figure 5 – The average step test response for the open loop system. The results of numerous tests were averaged to produce this result. The characteristics of the system were determined by finding the equations that describe the average response of the system. The following data was extracted: Gain = 26 Damping Factor $\zeta = 0.204$ Natural Oscillation Frequency $\omega_n = 91.29$Hz 2% Settling Time = 0.214s

The relatively high gain and settling time along with the low damping factor were identified as the main characteristics that needed to be improved by any sort of control circuitry that was to be implemented. Using the data obtained from the initial step tests a second order controller was designed to effectively improve the system. Once the controller was built, more step tests were performed and the results analysed. The results appear in figure 6 below.

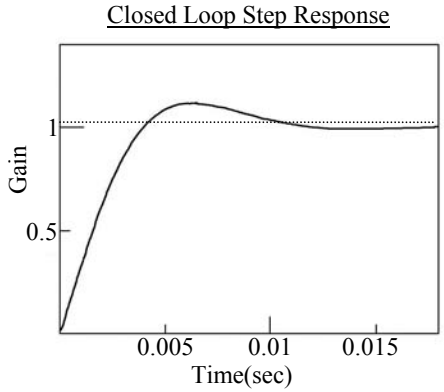

Figure 6 – The step response for the closed loop system with the implemented second order controller. The response and characteristics were determined using the same process as used for the open loop test. From the open loop tests the areas identified for improvement were gain, damping factor and settling time. From the new graph it is clear that large improvements were achieved in all the areas of focus. Gain = 1.078, $\zeta = 0.615$, $\omega_n = 498.126$Hz, 2% Settling Time = 0.013s.

By reducing some of the time constants present in the system, greater speed increases would be possible. However by reducing these time constants the system would be more unstable.

Also the system is fast enough for the application so no further speed increase is necessary.

4. FORCE FEEDBACK MECHANISM

As mentioned before phase is used to measure the crystal's proximity to a surface. For this reason accurate phase measurement is imperative to the force feedback control system. There are numerous different techniques for phase detection ranging from simple mathematical techniques to complicated signal analysis. For simplicity the phase detector used was a simple differential operational amplifier circuit. This circuit multiplies the voltage difference between inputs by a preset value determined by external resistors. This circuit will output a sine wave of varying amplitudes depending on the phase between the two input signals.

Due to the fact that this phase detector cannot discern between lagging and leading phase the system was operate away from the zero phase region. As the phase is deliberately set to zero in the previous loop to reduce the rectifier ripple a phase offset is added before they were measured. The control system appears below in figure 7.

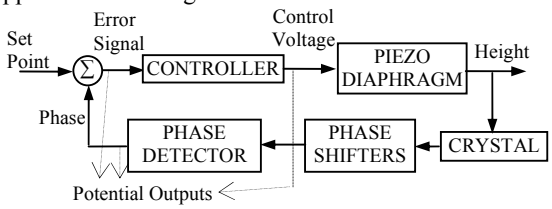

Figure 7 – The complete piezoelectric diaphragm control system. Shown are three potential measurement outputs for the system. The output from the phase detector and the error signal are very similar as the only difference would be due to any gains in the differential op amp. The diaphragm control voltage would give the best representation of ground motion at lower frequencies. At higher frequencies where more errors appear in the loop due to the system struggling to maintain the correct displacement, the other outputs might provide a better idea of actual ground motion. Again, all components external to the controller were grouped together to obtain a G(s) for the system. This G(s) is then used to design the controller.

As with the frequency locking loop, the controller was designed by first grouping together all external components as a g(s). Numerous step test results were analysed and averaged to ascertain a relative average response for the open loop system. The average response with its corresponding system characteristics appears below in figure 8.

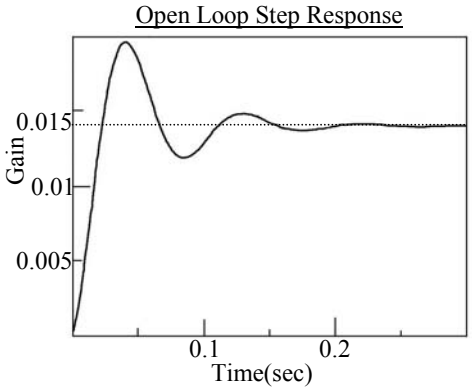

Figure 8 – Open loop response for the piezoelectric bimorph diaphragm control system. Again the system is slow and oscillatory with a low damping factor. As expected the response is faster than the amplitude response. For this result the Gain = 0.014, $\zeta = 0.204$, $\omega_n = 91.29$Hz 2% Settling Time = 0.214s

As expected the response is faster than the amplitude locking loop as the phase responds a lot more quickly. It is not however as fast as expected and this is due to the slow response of the piezoelectric diaphragm. The system is also still quite oscillatory and has a particularly low damping factor. These two problems, as well as the need to maximise system speed to increase effective bandwidth became the principle considerations in designing the controller. A second order controller was designed and implemented, the system was then tested again and the average results appear below in figure 9.

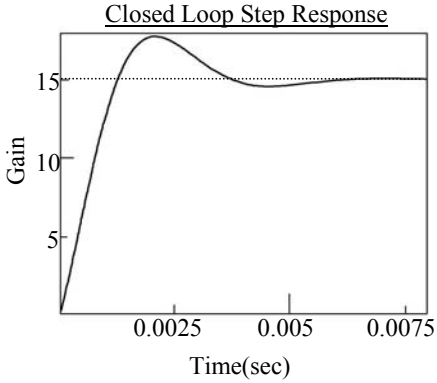

Figure 9 – The averaged step tests for the closed loop system for the piezoelectric diaphragm control system. The tests show that in close loop the system is much more stable and faster than the open loop. The Damping factor was improved and the gain increased to more suitable levels. Gain = 15.04, $\zeta = 0.507$, $\omega_n = 1458.04$Hz, 2% Settling Time = 0.0054s

The results of these tests indicate that the control systems are fast enough and stable enough to enable the entire system to perform as a seismometer and to test the basic principles behind the design of the

device. Further increases in speed and stability may be possible with further analysis and design but for the current requirements these control systems proved more than adequate.

5. RESULTS

The completed device was now tested against two known devices, an ADXL05 silicon MEMS accelerometer and an exploratory geophone. The devices were mounted on a loudspeaker drive capable of low frequency operation. Ground motion was simulated by driving the speaker with signals of different frequency and magnitude. Tests were performed to determine the bandwidth, low noise capability and the sensitivity of the seismometer.

For each frequency the output of the accelerometer and the geophone were compared to the control signal to the piezoelectric diaphragm in the tuning fork seismometer. The noise floor of each device was measured and compared to the outputs to obtain a signal to noise ratio for each frequency for each device.

The first test showed that the tuning fork seismometer follows the other device's response at lower frequencies. The expected roll off frequency of around 180Hz from the step tests was confirmed by the test. The geophone response also died out at these frequencies but the accelerometer output confirmed that the speaker was still moving. Due to the small accelerations at low frequencies the drive signal to the speaker was maximised for frequencies below 1 Hz. Oscilloscope screen shots of the seismometer response at these low frequencies appears below in figure 10.

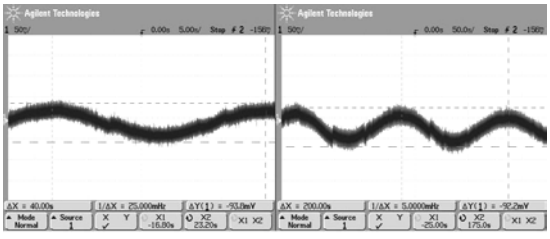

Figure 10 – Oscilloscope screen shots of the tuning fork seismometer's response at 25mHz and 5mHz. The seismometer may be able to function at lower frequencies and theoretically down to DC but 50sec per division was the longest time division available on the oscilloscope. There was no discernable response from either of the other devices at these low frequencies due to the low loud speaker acceleration.

Although much more sensitive than the accelerometer, the tuning fork seismometer had a worse average signal to noise ratio than the geophone. The poor mechanical sensitivity of the seismometer due to the low mass and high spring constant of the piezoelectric diaphragm was improved by adding mass to the diaphragm to increase the mass in the system. Although more sensitive, the noise signal of the seismometer output also increased. On closer analysis of the seismometer and geophone signals it was notice that there was in fact substantial correlation between the signals, indicating background seismic noise.

To reduce this background seismic noise the testing equipment could be isolated from all external noise. However as there were two correlated signals it was decided to use mathematical techniques to separate the noise signal. The mathematical techniques used are described in detail in the book 'Engineering Applications of Correlation and Spectral Analysis' by Bendat et al [3].

The technique uses the coherence, or fraction of the power of one signal that also appears in another signal, to determine which components of the signals are unique to each signal and which components of the signals are common to both of the signals. For a seismic signal S(t) the system can be illustrated by the block diagram in figure 11 below.

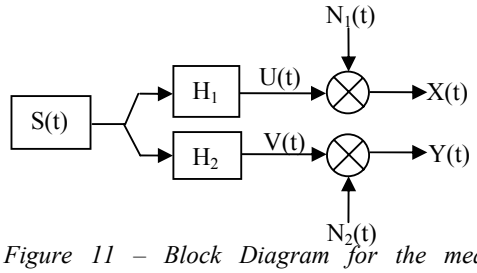

Figure 11 – Block Diagram for the measurement process. S(t) is the seismic signal. $H_{1,2}$ are the transfer functions for each of the sensors which produces a voltage dependant on the seismic signal. $N_{1,2}(t)$ are the two independent noise signals. X(t) is the measured signal from the geophone and Y(t) is the measured signal from the seismometer.

Coherence is defined as follows,

$$\textbf{Coherence: } \gamma^2_{XY}(\omega) = \frac{(G_{XY}(\omega))^2}{G_{XX}(\omega)\, G_{YY}(\omega)}$$

Where G_{XY} is the cross spectral density of signal X and signal Y and Gxx is the power spectral density of signal X. Coherence is then calculated by averaging the cross spectral density and power spectral densities from many different samples of signal X and Y. G_{XX} and G_{YY} can be broken up into their signal components as follows.

$$G_{XX}(\omega) = G_{UU}(\omega) + G_{N1N1}(\omega) = |H_1|^2 G_{SS}(\omega) + G_{N1N1}(\omega)$$

$$G_{YY}(\omega) = G_{VV}(\omega) + G_{N2N2}(\omega) = |H_2|^2 G_{SS}(\omega) + G_{N2N2}(\omega)$$

In order for the required signal components to be extracted the very small geophone noise is assumed to be zero. This eliminates one of the variables and

allows the equations to be solved. Small as the geophone noise is, the 50 Hz component of the signal was reduced by filtering to further reduce the noise of the sensor. The noise of the tuning fork seismometer can now be extracted as follows.

$$\gamma^2_{XY}(\omega) = \gamma^2_{SY}(\omega) = \frac{|H_2 G_{SS}(\omega)|^2}{G_{SS}(\omega)\, G_{YY}(\omega)} = \frac{G_{VV}(\omega)}{G_{YY}(\omega)}$$

$$G_{VV}(\omega) = G_{YY}(\omega)\, \gamma^2_{XY}(\omega)$$

$$G_{N2N2}(\omega) = G_{YY}(\omega)\, (1 - \gamma^2_{XY}(\omega))$$

Numerous sets of data were recorded, analysed and averaged so that the various relevant results could be calculated. These results were then used as shown in the equations above to extract the noise signal and the recorded seismic signals from the recorded data for the tuning fork seismometer. Graphs of the results appear below in figure 12.

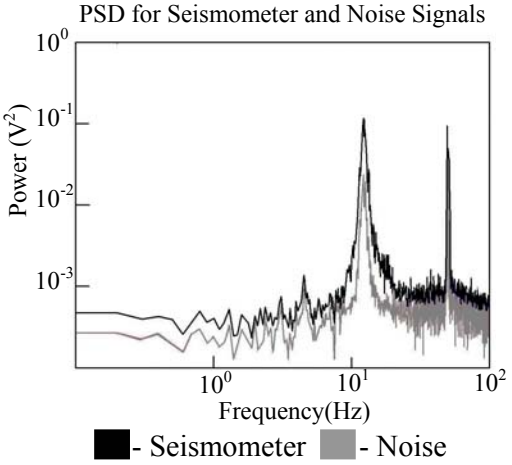

Figure 12 – Graphs of the recorded power spectral density for the seismometer and the extracted noise signal. The power is given in volts squared and is the actual reading for each reading squared. The main noise signal is at 50 Hz. The noise spike at 14 Hz is due to a phase shift between the two signals resulting in an imperfect correlation in some cases. Increasing the number of samples would further decrease this spike leaving just the 50 Hz signal as the chief source of noise.

From the first result the transfer function H_1 for the geophone can be calculated by comparing the output of the geophone with that of the accelerometer. H_1 can then be used to calculate the actual size of the seismic signal. The seismic signal can then in turn be used to calculate H_2 the tuning fork seismometer transfer function. Sensitivity can now be determined using the equations above.

Average sensitivity of the seismometer is calculated to be 2.7919V/m.s^{-2}. With the recorded noise level of the 50 Hz signal having a magnitude of 0.298V the minimum measurable acceleration will be 0.106m.s^{-2}.

6. CONCLUSIONS AND DISCUSSIONS

This paper has proved that the concept of using a tuning fork crystal and piezoelectric diaphragm in a force feedback system can function as a seismometer. The bandwidth of the device is shown to be DC to about 200Hz with an average sensitivity of about 10mg.

Although good results were achieved further improvements are possible. Reducing the 50 Hz noise would dramatically improve the system as the next recorded noise signal is about 100 times smaller than the 50 Hz noise signal. Alterations to the mechanical sensitivity and frequency operating point would also increase sensitivity; however the slow response of the piezoelectric diaphragm would have to be improved to realise these improvements. Increasing the speed of the piezoelectric diaphragm response would also increase the bandwidth of the device.

REFERENCES

[1] Barzilai, A., VanZandt, T., Pike, T., Manion, S. and Kenny, T. "Improving the Performance of a Geophone through Capacitive Position Sensing and Feedback", Conference Proceedings, American Society of Mechanical Engineers International Conference, Nov. 1998.

[2] Grober, R.D., Acimovic, J., Schuck, J., Hessman, D., Kindlemann, P., Hesphana, J., Morse, S.A., Karrai, K., Tiemann, I., and Manus, S. Fundamental limits to force detection using quartz tuning forks, Rev. Sci. Instrum. 71 (7): 2776-2780, 2000

[3] Bendat J.S and Piersol A.G, *Engineering Applications of Correlation and Spectral Analysis,* 2nd ed. (Wiley, New York,1993)